

LETTER TO THE JOURNAL

Engineering heavy chain antibody-drug conjugates against solid tumors for a one-shot kill

The inefficient tumor penetration of conventional antibodies has hampered the effective use of antibody-drug conjugates (ADCs) against solid tumors [1–5]. Compared with full-length antibodies and single-chain variable fragment (scFv), nanobodies (Nbs) have much smaller molecular weights, allowing them to achieve deeper tissue penetration, and they have become an attractive candidate platform for conjugating small-molecule drugs and tracers because of their favourable thermostability and high bioengineering potential [6, 7]. However, the clinical application of Nb-based ADCs is limited due to the short half-life of the Nbs [8]. This letter reports the identification and biological characterization of an innovative heavy chain antibody (HCAb)-drug conjugate based on a Nb from a trophoblast cell surface antigen 2 (TROP2)-immunized alpaca. HCAb has been verified to possess fast and efficient penetration into tumor tissues as its molecular weight (~80 kDa) is half that of a classical antibody (~150 kDa) [9]. We mutated the sites serine 149 and lysine 200 of the HCAb to cysteine, and then coupled the antimitotic agent monomethyl auristatin E (MMAE) to the engineered surface cysteine with the proteolyzable linker maleimidocaproyl-valine-citrulline-p-aminobenzoyloxycarbonyl (MC-Val-Cit-PAB), resulting in a conjugate abbreviated as C3 ADC (Figure 1A). Compared with conventional RS7 ADC, C3 ADC exhibits exceptionally higher stability, much deeper tumor penetration, significantly greater tumor uptake, and faster accumulation at tumor sites, leading to improved tumor inhibition. Notably, the engineered Nb-drug conjugate exhibits potent ‘one-shot kill’ efficacy against solid tumors. This study presents, for the first time, a HCAb drug conjugate strategy that can efficiently reduce tumor burden.

We screened and identified the TROP2 Nb following our protocol for specific Nbs (Supplementary Figure S1).

List of abbreviations: ADC, Antibody-drug conjugates; CLSM, confocal laser scanning microscopy; DAR, drug-to-antibody ratio; FDA, the United States Food and Drug Administration; HCAb, heavy chain antibody; Nbs, Nanobodies; MMAE, monomethyl auristatin E; TROP2, trophoblast cell surface antigen 2.

To enhance the expression and extend the half-life, the Nb was fused with an hFc domain, termed C1 HCAb. C1 HCAb-DyLight 633 was more significantly endocytosed by TROP2-overexpressing MDA-MB-231 cells in a time-dependent manner than RS7-DyLight 633 (Figure 1B and Supplementary Figure S2). In contrast, Huh7 cells without TROP2 expression had poor internalization of C1 HCAb (Supplementary Figure S3). These results indicated that C1 HCAb can be selectively taken up by tumor cells expressing high levels of TROP2.

We then performed site-directed mutagenesis to design a site-specific mutant antibody, C3 HCAb (Supplementary Figures S4–S5). Here, lysosomal-cleavable MC-Val-Cit-PAB was used as a linker and the antimitotic agent MMAE was coupled to the engineered surface of cysteine, forming the conjugate C3 ADC. For the positive ADC control, site-directed mutation of the antibody portion of the FDA-approved ADC Trodelvy (sacituzumab) (hRS7) was performed at the same site, and the antibody was conjugated with the same linker and payload. The drug-to-antibody ratio (DAR) of C3 ADC was calculated by hydrophobic interaction chromatography. C3 ADC (DAR = 3.96) exhibited a homogeneous conjugation profile, suggesting the superior accessibility of the mutated C3 HCAb with respect to site-specific conjugation (Figure 1C, Supplementary Figures S6–S7). Next, we quantified the affinity between C3 HCAb and hTROP2 using SRP (surface plasmon resonance), revealing a KD value of 6.18 nmol/L (Figure 1D), indicating that C3 exhibited good affinity. Furthermore, C3 ADC demonstrated favorable thermostability and remarkable stability (Figure 1E, Supplementary Figure S8). Cathepsin B did not impact C3 HCAb but facilitated over 70% MMAE release from C3 ADC within 3 h (Supplementary Figure S9).

The ability of HCAb to bind to cell surface antigens and be internalized was assessed. C3 ADC achieved an internalization rate of approximately 50% in pancreatic cancer cell (BxPC-3) and triple-negative breast cancer cells (MDA-MB-231) within 3 h (Figure 1F, Supplementary Figure S10).

This is an open access article under the terms of the [Creative Commons Attribution-NonCommercial-NoDerivs](https://creativecommons.org/licenses/by-nc-nd/4.0/) License, which permits use and distribution in any medium, provided the original work is properly cited, the use is non-commercial and no modifications or adaptations are made.

© 2024 The Author(s). *Cancer Communications* published by John Wiley & Sons Australia, Ltd on behalf of Sun Yat-sen University Cancer Center.

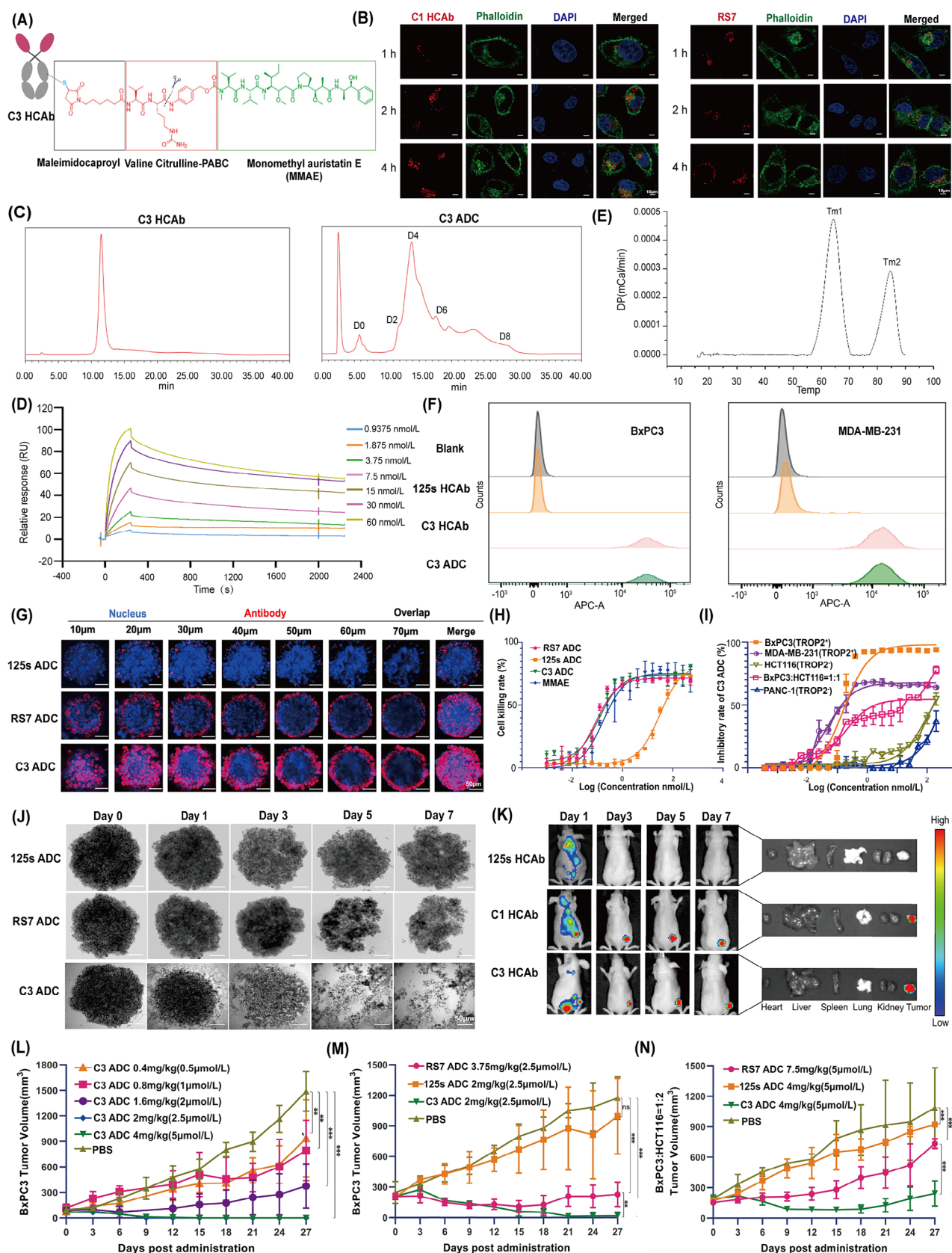


FIGURE 1 Engineering anti-TROP2 heavy chain ADCs. (A) Schematic of C3 ADC. (B) The process of C1 HCAb and RS7 internalization by TROP2-positive MDA-MB-231 cells. (C) Hydrophobic interaction chromatography (HIC) analysis of C3 ADC. (D) Thermal stability of C3 ADC as measured by differential scanning calorimetry (DSC). (E) Characterization of the affinity of C3 ADC for hTROP2 using BIAcore analysis. (F) Flow cytometry assessment of the binding abilities of 125s HCAb, C3 HCAb and C3 ADC to BxPC3 and MDA-MB-231 cells. (G)

Penetration of C3 ADC, RS7 ADC and 125s ADC in BxPC3 tumour spheroids, as determined by confocal microscopy. (H) In vitro toxicity of ADCs in MDA-MB-231 cells. (I) In vitro toxicity of C3 ADC in cancer cells with different percentage of TROP2 expression. (J) Penetration of 125s ADC, RS7 ADC and C3 ADC into BxPC3 tumor spheroids and their lysis abilities. (K) Time-lapse in vivo NIR FL images of nude mice and *ex vivo* NIR FL images of major organs and tumors 7 days after injection of 125s HCAb, C1 HCAb and C3 HCAb. (L) in vivo concentration-dependent antitumor activity of a single dose of C3 ADC in the BxPC3 xenograft model (The curves of 2 mg/kg and 4 mg/kg almost overlapped). (M) Efficacy of C3 ADC against large tumors. When the mean volume of the implanted BxPC3 tumors was greater than 250 mm³, C3 ADC (2 mg/kg) was administered. (N) in vivo antitumor activity of a single dose of C3 ADC in a heterogeneous tumor model (1×10⁶ TROP2⁺ BxPC3 cells mixed with 2×10⁶ TROP2⁻ HCT116 cells). Results are presented as mean ± s.d. Significant differences were assessed using a two-way ANOVA with multiple comparisons (L, M, N). n = 5-6, ***p* < 0.01, and ****p* < 0.001.

We evaluated the In vitro tumor penetration of the conjugates using 3-dimensional (3D) tumor spheroids composed of BxPC-3 cells. The spheroids were incubated with RS7 ADC, C3 ADC and 125s-vc-MMAE (a nonbinding control ADC, abbreviated as 125s ADC). Strong fluorescence from the RS7 ADC was observed on the surface of the tumor organoids. However, the fluorescence decreased in the centre, indicating that RS7 could not penetrate the inner tumor organoids. In contrast, the C3 ADC group exhibited remarkably widespread fluorescence signals throughout the tumor organoids, suggesting that the C3 ADC could penetrate deep into the solid tumor and be more extensively distributed (Figure 1G).

The rapid internalization and lysosomal degradation of receptors could contribute to effective ADC delivery and intracellular release of the payload in tumor cells. The majority of the internalized C3 ADCs were colocalized with the lysosomal marker LAMP-2, suggesting that they were successfully trafficked to lysosomes, as expected (Supplementary Figure S11). TROP2-positive (TROP2⁺) tumor cells were treated with ADCs for 3 days. The C3 ADC and RS7 ADC- exhibited similar and potent In vitro efficacy on MDA-MB-231 cells (Figure 1H and Supplementary Figure S12A). C3 ADC induced a dose-dependent increase in cell apoptosis in BxPC3 cells, whereas no significant increase of apoptotic cells was observed after treatment with 125s ADC (Supplementary Figure S13). The potent killing was also observed in a heterogeneous mixture of BxPC3 and HCT116 cells (50% TROP2⁺ cells) with C3 ADC (Figure 1I and Supplementary Figure S12B). Conversely, no inhibitory effect was observed on low TROP2-expressing cells, such as HCT116 and PANC-1 cells.

In BxPC3 tumor spheroid models, the negative control 125s ADC mildly affected spheroid integrity, while RS7 ADC caused marked edge disruption by day 5. Interestingly, C3 ADC treatment led to significant fragmentation, which was evident on day 3, and full cleavage by day 5 (Figure 1J).

The specific accumulation of C3 HCAb in the tumor site was monitored in a BxPC3 xenograft model (Figure 1K).

C3 ADC exhibited potent dose-dependent antitumor activity in tumor xenografts, which were completely cleared by a single dose of 2 mg/kg administration (Figure 1L). There were no obvious signs of adverse events in any treatment groups (Supplementary Figure S14). After a single administration of C3 ADC, tumor proliferation was inhibited and apoptosis was induced, with marked regression of relatively large tumors observed compared to RS7 ADC (Supplementary Figure S15 and Figure 1M). In addition, in the BxPC3-Luc peritoneal model, a significant decrease in bioluminescence signal was observed in C3 ADC-treated mice (4 mg/kg, single injection, intravenously) after one week (Supplementary Figure S16). C3 ADC also significantly delayed MDA-MB-231 tumor growth and showed better in vivo efficacy than RS7 ADC (Supplementary Figure S17). The above results indicate that C3 ADC exhibits powerful antitumor activity against pancreatic and triple-negative breast tumor xenografts.

MMAE is a cell membrane-permeable toxin with bystander effects and a good substrate for drug efflux pumps. In the heterogeneous tumor model (1×10⁶ TROP2⁺ BxPC3 cells mixed with 2×10⁶ TROP2⁻ HCT116 cells), a single administration of C3 ADC markedly reduced tumor size (Figure 1N, Supplementary Figure S18). C3 ADC showed an enhanced bystander killing effect, which has been speculated to be closely related to the efficient deep penetration ability of C3 ADC into tumors. In addition, C3 ADC is well tolerated and has no obvious in vivo toxicity (Supplementary Figures S19-S20).

In summary, our work demonstrates that a HCAb-based ADC, C3 ADC, exhibits advantages such as slight side effects, superior stability, rapid accumulation at tumor sites, and deep tumor penetration. Compared with previously reported TROP2-targeted Nb-based ADC [10] (Supplementary Table S1), this study presents, for the first time, a HCAb drug conjugate strategy with a potent 'one-shot kill' capability against large solid tumors, even those that are heterogeneous. This work provides important technical methods and a theoretical basis for ADC development and precise cancer treatment.

AUTHOR CONTRIBUTIONS

Ningshao Xia, Wenxin Luo and Xiaowen Yan are jointly corresponding authors. Ningshao Xia supervised and revised the manuscript. Wenxin Luo and Xiaowen Yan conceived the study, designed and supervised the experiments. Xue Liu, Wenjing Ning and Lei Wang designed and conducted the studies, analysed data, and drafted the manuscript. Han Liu and Yang Zhao performed ADCs preparation and analysis. Xiaojing Qin, Lin Xu and Xiaoqing Chen contributed to the in vitro experiments. Hongye Zeng and Yunlong Ren conducted part of the in vivo animal experiments. Yuanzhi Chen, Fentian Chen and Jixian Tang performed antibody screening and expression. All authors read and approved the final manuscript.

ACKNOWLEDGMENTS

Not applicable.

CONFLICT OF INTEREST STATEMENT

The authors declare no potential conflicts of interest.

FUNDING INFORMATION

This work was supported by the National Natural Science Foundation of China (No. 32070940, 82202500, 22074127 and 22193053), the Postdoctoral Innovation Talents Support Program (No. BX20220189).


DATA AVAILABILITY STATEMENT

The data that support the findings of this study are available from the corresponding author upon reasonable request.

ETHICS APPROVAL AND CONSENT TO PARTICIPATE

Animal experiments containing cell line-derived xenografts were carried out in accordance with the approval of the Institutional Animal Care and Use Committee at Xiamen University (XMULAC20200191) and in accordance with the Guide for the Care and Use of Laboratory Animals.

Xue Liu^{1,2}
Wenjing Ning^{1,2}
Lei Wang³
Han Liu^{1,2}
Hongye Zeng^{1,2}
Xiaojing Qin^{1,2}
Yuanzhi Chen^{1,2}
Fentian Chen^{1,2}
Lin Xu^{1,2}
Yang Zhao³
Xiaoqing Chen^{1,2}
Jixian Tang^{1,2}

Yunlong Ren^{1,2}
Xiaowen Yan^{3,4}
Wenxin Luo^{1,2}
Ningshao Xia^{1,2} 

¹State Key Laboratory of Vaccines for Infectious Diseases, Xiang An Biomedicine Laboratory, School of Public Health, Xiamen University, Xiamen, Fujian, P. R. China

²National Institute of Diagnostics and Vaccine Development in Infectious Diseases, State Key Laboratory of Molecular Vaccinology and Molecular Diagnostics, National Innovation Platform for Industry-Education Integration in Vaccine Research, the Research Unit of Frontier Technology of Structural Vaccinology of Chinese Academy of Medical Sciences, Xiamen University, Xiamen, Fujian, P. R. China

³Department of Chemistry and the MOE Key Laboratory of Spectrochemical Analysis & Instrumentation, College of Chemistry and Chemical Engineering, Xiamen University, Xiamen, Fujian, P. R. China

⁴Innovation Laboratory for Sciences and Technologies of Energy Materials of Fujian Province (IKKEM), Xiamen, Fujian, P. R. China

Correspondence

Ningshao Xia and Wenxin Luo, State Key Laboratory of Vaccines for Infectious Diseases, Xiang An Biomedicine Laboratory, School of Public Health, Xiamen University, Xiamen 361102, Fujian, P. R. China.

Email: nsxia@xmu.edu.cn and wxliao@xmu.edu.cn

Xiaowen Yan, Department of Chemistry and the MOE Key Laboratory of Spectrochemical Analysis & Instrumentation, College of Chemistry and Chemical Engineering, Xiamen University, Xiamen 361005, Fujian, P. R. China.

Email: xwyan@xmu.edu.cn

Xue Liu, Wenjing Ning, and Lei Wang made equal contributions to this work.

ORCID

Ningshao Xia  <https://orcid.org/0000-0003-0179-5266>

REFERENCES

1. Dumontet C, Reichert JM, Senter PD, Lambert JM, Beck A. Antibody-drug conjugates come of age in oncology. *Nat Rev Drug Discov.* 2023;22(8):641–661.
2. Tarantino P, Ricciuti B, Pradhan SM, Tolane SM. Optimizing the safety of antibody-drug conjugates for patients with solid tumours. *Nat Rev Clin Oncol.* 2023;20(8):558–576.
3. Passaro A, Jänne PA, Peters S. Antibody-Drug Conjugates in Lung Cancer: Recent Advances and Implementing Strategies. *J Clin Oncol.* 2023;41(21):3747–3761.
4. Tsuchikama K, Anami Y, Ha SYY, Yamazaki CM. Exploring the next generation of antibody-drug conjugates. *Nat Rev Clin Oncol.* 2024;21(3):203–223.

5. Minchinton AI, Tannock IF. Drug penetration in solid tumours. *Nat Rev Cancer*. 2006;6(8):583–592.
6. Strack R. Nanobodies made versatile. *Nat Methods*. 2023;20(1):37.
7. Muyldermans S. Nanobodies: natural single-domain antibodies. *Annu Rev Biochem*. 2013;82:775–797.
8. Wu Y, Li Q, Kong Y, Wang Z, Lei C, Li j, et al. A highly stable human single-domain antibody-drug conjugate exhibits superior penetration and treatment of solid tumors. *Mol Ther*. 2022;30(8):2785–2799.
9. Gan X, Shan Q, Li H, Janssens R, Shen Y, He Y, et al. An anti-CTLA-4 heavy chain-only antibody with enhanced Treg depletion shows excellent preclinical efficacy and safety profile. *Proc Natl Acad Sci U S A*. 2022;119(32):e2200879119.
10. Xu C, Zhu M, Wang Q, Cui J, Huang Y, Huang X, et al. TROP2-directed nanobody-drug conjugate elicited potent antitumor effect in pancreatic cancer. *J Nanobiotechnology*. 2023;21(1):410.

SUPPORTING INFORMATION

Additional supporting information can be found online in the Supporting Information section at the end of this article.